PM/98-20
CPT-98/P3677
THES-TP 98/06
hep-ph/9807563
July 1998

Glue constraining asymmetries in W, γ or Z production at CERN LHC[†]

P. Chiappetta[a], G.J. Gounaris[b], J. Layssac[c] and F.M. Renard[c]

[a]Centre de Physique Théorique, UPR 7061, CNRS Luminy, F-13288 Marseille, France

[b]Department of Theoretical Physics, University of Thessaloniki,
Gr-54006, Thessaloniki, Greece.

[c]Physique Mathématique et Théorique, UMR 5825
Université Montpellier II, F-34095 Montpellier Cedex 5.

Abstract

We propose a class of forward-backward asymmetries with respect to the subprocess c.m. scattering angle in V+jet production at hadron colliders, with V being any of (W, Z, γ, H), which are directly proportional to the gluon distribution $g(x)$. The informations that these asymmetries can provide are complementary of those reachable from measurements of the transverse momentum and/or the rapidity distributions of a V in kinematical regimes where gluon scattering subprocesses dominate. The accuracy which can be reached in the W, Z and γ cases, at the upgraded Tevatron and at LHC, should allow a considerable improvement of our knowledge of the gluon distribution function, especially at large x.

PACS: 12.38.Bx, 14.70.Dj, 24.85.+p, 12.38.Qk

[†]Partially supported by the EC contract CHRX-CT94-0579, and by the NATO grant CRG 971470.

1 Introduction

One difficulty in our effort to test the Standard Model (SM) at a hadronic collider, and search for any new physics (NP) beyond it, is due to the uncertainties pertaining to the gluon distribution [1, 2, 3]. Remembering for example, that $gg \to H$ provides the dominant contribution to H-production at LHC in the region of $100\ GeV \lesssim m_H \lesssim 800\ GeV$ [4, 5], we infer that a good knowledge of the gluon distribution is necessary for studying the properties of the Higgs particle and precisely estimating the backgrounds.

The main constraints to the gluon distribution inside a nucleon at present, arise from DIS measurements which probe the low x range [6], and at higher x from measurements of the p_T distribution of a prompt photon produced in $pp \to \gamma X$ at $\sqrt{s} = 23\ GeV$ WA70 [7], and in $pBe \to \gamma X$ at $p_{lab} = 530\ GeV$ [8], and also from heavy flavor production [9]. The combinations of subprocess cross sections contributing to prompt photon production are always forward-backward symmetrical in the subprocess c.m., and consist of

$$\frac{d\hat{\sigma}(q\bar{q} \to \gamma g)}{d\hat{t}} \ , \tag{1}$$

and

$$\frac{d\hat{\sigma}(gq(\bar{q}) \to \gamma q(\bar{q}))}{d\hat{t}} \ + \ \frac{d\hat{\sigma}(q(\bar{q})g \to \gamma q(\bar{q}))}{d\hat{t}} \ , \tag{2}$$

as well as of subprocess cross sections in which the photon comes from a quark or gluon fragmentation. The sensitivity of such measurements on $g(x)$, arises from the fact that for pp or proton-Nucleus scattering, the second subprocess (2) dominates over most of the p_T region [1], provided that the produced photon is constrained to be sufficiently isolated [10], in order to reduce the magnitude of the fragmentation contribution.

Further information on $g(x)$, from such forward-backward symmetrical subprocesses, could arise at LHC and the upgraded Tevatron. It has been shown [11] that a detailed measurement of the rapidity distributions of an inclusively produced gauge boson W, Z or γ, accompanied by a hard jet might provide an accurate determination of the gluon structure function. In principle, the same kind of information could also arise from Higgs+jet production, but the expected statistics is very limited in this case. Since the theoretical treatment of any (V+jet) production for ($V \ = \ W, \ Z, \ \gamma, \ H$) is very similar, we consider below all these cases together.

Thus, if in a (V+jet) pair production, we restrict ourselves to measurements of the p_T and/or rapidity distributions of V, then we are only sensitive to the combinations of subprocess cross sections[1]

$$\frac{d\hat{\sigma}(q\bar{q} \to Vg)}{d\hat{t}} \ , \tag{3}$$

and

$$\frac{d\hat{\sigma}(gq(\bar{q}) \to Vq(\bar{q}))}{d\hat{t}} \ + \ \frac{d\hat{\sigma}(q(\bar{q})g \to Vq(\bar{q}))}{d\hat{t}} \ , \tag{4}$$

[1]For the moment we disregard contribution from photon fragmentation, to which we come back below.

while for Higgs production we also get contributions from

$$\frac{d\hat{\sigma}(gg \to Hg)}{d\hat{t}} \quad . \tag{5}$$

These combinations of the subprocess cross sections lead to (V+jet) distributions which are symmetrical with respect to the (V+jet) c.m. rapidity $\bar{y}$, as well as with respect to $\cos\theta^*$, where θ^* is the subprocess c.m. scattering angle.

We want to stress in this paper that in addition to these quantities, there exist a contribution proportional to the combination

$$\frac{d\hat{\sigma}(gq(\bar{q}) \to Vq(\bar{q}))}{d\hat{t}} \quad - \quad \frac{d\hat{\sigma}(q(\bar{q})g \to Vq(\bar{q}))}{d\hat{t}} \quad , \tag{6}$$

of the subprocess cross sections, which induces (V+jet) distributions which are *anti-symmetric* with respect to $\bar{y}$, as well as with respect to $\cos\theta^*$. It turns out that these distributions are directly sensitive to $g(x)$ (in fact they are directly proportional to it) and supply independent additional information, especially in the large x range, which to our knowledge has not been used so far, certainly due to the lack of statistics in present colliders. Of course, they also provide new information for the other parton distributions. The aim of the present paper is to study these quantities. To achieve this goal we construct for each (V+jet) final state, a forward-backward asymmetry with respect to $\cos\theta^*$, which is thus a function of the subprocess energy squared $\hat{s} \equiv M^2$, as well as an odd function of the rapidity $\bar{y}$ of the center of mass.

In calculating the aforementioned asymmetries for the $V = W,\ Z,\ H$ cases, our philosophy is to keep the leading QCD contribution for the (V+jet) final state, and include the antenna pattern effect arising from the additional (V+jet+ soft gluon) final state integrated in a suitable phase space region [12, 13], as a rough estimate of higher order QCD corrections. It turns out that the exact size of this antenna phase space region, is not very important for the considered asymmetries. For the (γ+jet) case, we also include the photon fragmentation contribution, whose effect is again not very important, provided that a sufficiently strong isolation cut is imposed on the produced photon. Such an isolation is anyway desired, in order to increase the sensitivity of the above asymmetry on the gluon distribution.

The content of the paper is the following. In Section 2, the formalism is presented containing the definition of the forward-backward asymmetry for the V+jet production, and including also discussions of the possible antenna pattern effects and the photon fragmentation contribution. In Sect. 3 the sensitivity of the above asymmetry to the gluon distribution is discussed, while the conclusions are given in Sect. 4. Finally the subprocess cross sections and quark distributions for the various V cases, are given in the Appendix.

2 Formalism

2.1 The V+jet contribution.

The generic subprocess contributing to the $pp \to V\ jet\ ...$ ($V = W,\ Z,\ \gamma,\ H$) cross section (apart from the photon fragmentation case discussed separately), is written as

$$a(p_1)\ +\ b(p_2)\ \to\ V(p_3)\ +\ c(p_4)\ \ , \tag{7}$$

where the momenta are indicated in parentheses and the masses of the partons ($a,\ b,\ c$) are neglected. As usual $\hat{s} = (p_1 + p_2)^2$, $\hat{t} = (p_3 - p_1)^2$, $\hat{u} = (p_3 - p_2)^2$. We also define $\tau = \hat{s}/s$, where s is the LHC (or Tevatron) c.m. energy-squared. The rapidity $\bar{y}$ of the c.m. of the (V+jet) subprocess determines the momentum fractions of the incoming partons through

$$x_a = \sqrt{\tau} e^{\bar{y}} \quad , \quad x_b = \sqrt{\tau} e^{-\bar{y}}\ , \tag{8}$$

while the scattering angle in the c.m. of the same subprocess satisfies[2]

$$\cos\theta^* \ = \ \frac{\hat{u} - \hat{t}}{\hat{u} + \hat{t}}\ \ . \tag{9}$$

The (V+jet) production cross section in pp collisions is given by

$$\begin{aligned}
\frac{d\sigma(pp \to V\ jet)}{d\tau d\bar{y} d\cos\theta^*} = \frac{\hat{s} - m_V^2}{2} \Bigg\{ & g(x_a, Q^2) g(x_b, Q^2) \frac{d\hat{\sigma}(gg \to Vg)}{d\hat{t}} \\
& + \widetilde{\Sigma}_V(x_a, x_b) \frac{d\hat{\sigma}(q\bar{q}' \to Vg)}{d\hat{t}} \\
& + \frac{1}{2}\left[g(x_a, Q^2)\Sigma_V(x_b) + \Sigma_V(x_a) g(x_b, Q^2) \right] \left[\frac{d\hat{\sigma}(gq \to Vq)}{d\hat{t}} + \frac{d\hat{\sigma}(qg \to Vq)}{d\hat{t}} \right] \\
& + \frac{1}{2}\left[g(x_a, Q^2)\Sigma_V(x_b) - \Sigma_V(x_a) g(x_b, Q^2) \right] \left[\frac{d\hat{\sigma}(gq \to Vq)}{d\hat{t}} - \frac{d\hat{\sigma}(qg \to Vq)}{d\hat{t}} \right] \Bigg\}\ ,
\end{aligned} \tag{10}$$

where (8, 9) should be used. In (10), $Q \simeq p_T/2$ is the usually preferred factorization scale of the distribution functions which mimic the next to leading order corrections. The $\Sigma_V, \widetilde{\Sigma}_V$ terms describe combinations of quark (antiquark) distributions weighted by the quark electromagnetic or weak charge, while $d\hat{\sigma}$ denote the correspondingly normalized subprocess cross sections, for the various $V = H,\ W,\ Z,\ \gamma$ cases. These are given in the Appendix for a pp Collider, while for the $p\bar{p}$ Tevatron they should be modified in an obvious way.

The last two terms of eq.(10) have been constructed by combining the corresponding gluon×quark and the quark×gluon contributions in a symmetrical and an antisymmetrical parts. It is important to note that the last term in (10) is *antisymmetric* with respect to $\bar{y}$ or $\cos\theta^*$ for the Tevatron or LHC Colliders, while all other terms are symmetric in both these variables. This last term will therefore be washed out if we integrate over $\bar{y}$, as it always happens whenever we only look at the rapidity and/or p_T distribution

[2]For a collection of relevant kinematical formulae see *e.g.* Appendix A3 in [14].

of a single V or jet. It will also be washed out, in case we cannot discriminate V from the accompanying jet, and therefore also in dijet production. Particularly for the dijet case, we note that so long we cannot discriminate between a gluon and a quark jet, the $\cos\theta^*$-antisymmetric term in (10) vanishes identically, and only the symmetric part of (10) contributes. For studying therefore the last term in (10), which is the main purpose of the present paper, the two high p_T objects in the final state should be distinguishable, as *e.g.* in the case a W, Z or γ production, accompanied by a high p_T jet.

We next turn to the corrections to the various terms in (10), arising from soft gluon emission in the antenna approximation, and from photon fragmentation in case $V = \gamma$.

2.2 Adding the antenna pattern contribution.

The hadronic antenna patterns in $V = W,\ Z,\ \gamma$ + jet production have been shown to provide a valuable diagnostic tool for probing the nature of the underlying parton subprocess. They could also provide a good tool for distinguishing between conventional QCD and new physics production [15] (large E_T jet events in hadronic collisions, or large anomalous Q^2 events at HERA). Here the philosophy is different: in order to make our treatment more realistic, we add to the leading order calculation of the V+jet cross section, the contribution from the soft gluon emission. Thus, for each subprocess like in (7), we consider the corresponding subprocess

$$a(p_1) \ + \ b(p_2) \ \rightarrow \ V(p_3) \ + \ c(p_4) \ + \ g(k) \ . \tag{11}$$

The soft gluon emission in such subprocesses is controlled by the basic antenna pattern distribution [12]

$$[ij] \ = \ \frac{p_i \cdot p_j}{p_i \cdot k \ p_j \cdot k} \ , \tag{12}$$

which should be adequate for the description of gluonic minijets with energies k_0 much smaller than those of the hard jets [13].

The contribution from the (V+jet + soft gluon) production cross section in pp collisions is then given by (compare (10))

$$\begin{aligned}
& k_0 \, \frac{d\sigma(pp \rightarrow V \ jet)}{d\tau d\bar{y} d\cos\theta^* d^3k} = \frac{3\alpha_s(\hat{s} - m_V^2)}{8\pi^2} \ \cdot \\
& \left\{ g(x_a, Q^2) g(x_b, Q^2) \left([12] + [14] + [24] \right) \frac{d\hat{\sigma}(gg \rightarrow Vg)}{d\hat{t}} \right. \\
+ \ & \widetilde{\Sigma}_V(x_a, x_b) \left([14] + [24] - \frac{[12]}{9} \right) \frac{d\hat{\sigma}(q\bar{q}' \rightarrow Vg)}{d\hat{t}} \\
+ \ & \frac{1}{2} \left[g(x_a, Q^2) \Sigma_V(x_b) + \Sigma_V(x_a) g(x_b, Q^2) \right] \cdot \\
& \left[\left([12] + [14] - \frac{[24]}{9} \right) \frac{d\hat{\sigma}(gq \rightarrow Vq)}{d\hat{t}} + \left([12] + [24] - \frac{[14]}{9} \right) \frac{d\hat{\sigma}(qg \rightarrow Vq)}{d\hat{t}} \right] \\
+ \ & \frac{1}{2} \left[g(x_a, Q^2) \Sigma_V(x_b) - \Sigma_V(x_a) g(x_b, Q^2) \right] \cdot
\end{aligned}$$

$$\left[\left([12]+[14]-\frac{[24]}{9}\right)\frac{d\hat{\sigma}(gq\to Vq)}{d\hat{t}}-\left([12]+[24]-\frac{[14]}{9}\right)\frac{d\hat{\sigma}(qg\to Vq)}{d\hat{t}}\right]\Bigg\} \quad (13)$$

Neglecting all parton masses, except m_V, we use the notation $p_1^\mu=\sqrt{\hat{s}}/2(1,0,0,1)$, $p_2^\mu=\sqrt{\hat{s}}/2(1,0,0,-1)$ for the description of the momenta of the incoming partons a,b in their c.m. (compare (11)), and the notation

$$p_V^\mu = p_3^\mu=(E_{VT}\cosh y_V^*,\ p_T,\ 0,\ E_{VT}\sinh y_V^*)\ , \quad (14)$$
$$p_4^\mu = p_T(\cosh\eta_c^*,\ -1,\ 0,\ \sinh\eta_c^*)\ , \quad (15)$$
$$k^\mu = k_T(\cosh(\eta_c^*+\delta\eta),\ \cos(\delta\varphi),\ \sin(\delta\varphi),\ \sinh(\eta_c^*+\delta\eta))\ , \quad (16)$$

for the final state particles in the same frame [13]. Here $E_{VT}=\sqrt{m_V^2+p_T^2}$ gives the transverse energy of V, and $(y_V^*,\ \eta_c^*)$ denote the rapidities of $(V,\ c)$ in the (a,b)-c.m. frame. The final gluon is taken to be soft, which means

$$\Lambda_{QCD}\ll k_0\ll\sqrt{\hat{s}}/2,\ E_{VT}\cosh y_V^*,\ p_T\cosh\eta_c^*\ . \quad (17)$$

Note from (15, 16), that to the extent that $\delta\eta\ ,\ \delta\varphi$ are small, the rapidity and azimuthal angle of the minijet generated by the soft gluon are close to those of the hard jet generated by parton c; compare (11).

In terms of these variables the antenna pattern coefficients in (12) may be expressed as

$$[12] = \frac{2}{k_T^2}\ , \quad (18)$$
$$[14] = \frac{e^{\delta\eta}}{k_T^2\left[\cosh(\delta\eta)+\cos(\delta\varphi)\right]}\ ,\ , \quad (19)$$
$$[24] = \frac{e^{-\delta\eta}}{k_T^2\left[\cosh(\delta\eta)+\cos(\delta\varphi)\right]}\ , \quad (20)$$

while the phase space of the soft gluon is determined by

$$\frac{d^3k}{k_0} = k_T dk_T\ d\delta\eta\ d\delta\varphi\ . \quad (21)$$

Defining $\delta R\equiv\sqrt{\delta\eta^2+\delta\varphi^2}$, we choose to integrate the antenna activity contained in (13) in the region

$$\delta R_1\le\ \ \delta R\ \ \le\delta R_2\ , \quad (22)$$
$$k_{Tmin}\le\ \ k_T\ \ \le k_{Tmax}\ . \quad (23)$$

Adding then (10) and the result of integrating (13) we get

$$\frac{d\sigma(pp\to V\ jet)}{d\tau d\bar{y}d\cos\theta^*}=\frac{\hat{s}-m_V^2}{2}\Bigg\{g(x_a,Q^2)g(x_b,Q^2)I_{gg}\ \frac{d\hat{\sigma}(gg\to Vg)}{d\hat{t}}$$

$$
\begin{aligned}
&+ \quad \widetilde{\Sigma}_V(x_a,x_b) I_{q\bar{q}} \, \frac{d\hat{\sigma}(q\bar{q}' \to Vg)}{d\hat{t}} \\
&+ \quad \frac{1}{2}\left[g(x_a,Q^2)\Sigma_V(x_b) + \Sigma_V(x_a) g(x_b,Q^2) \right] I_{gq} \left[\frac{d\hat{\sigma}(gq \to Vq)}{d\hat{t}} + \frac{d\hat{\sigma}(qg \to Vq)}{d\hat{t}} \right] \\
&+ \quad \frac{1}{2}\left[g(x_a,Q^2)\Sigma_V(x_b) - \Sigma_V(x_a) g(x_b,Q^2) \right] I_{gq} \left[\frac{d\hat{\sigma}(gq \to Vq)}{d\hat{t}} - \frac{d\hat{\sigma}(qg \to Vq)}{d\hat{t}} \right] \Bigg\} \quad (24)
\end{aligned}
$$

where the antenna contribution is contained in the parameters

$$
\begin{aligned}
I_{gg} &= 1 + \frac{3\alpha_s}{2\pi^2} \ln\left(\frac{k_{Tmax}}{k_{Tmin}} \right) \left[\pi(\delta R_2^2 - \delta R_1^2) + \xi(\delta R_2,\ \delta R_1) \right] \ , \quad (25) \\
I_{gq} &= 1 + \frac{3\alpha_s}{2\pi^2} \ln\left(\frac{k_{Tmax}}{k_{Tmin}} \right) \left[\pi(\delta R_2^2 - \delta R_1^2) + \frac{4}{9}\xi(\delta R_2,\ \delta R_1) \right] \ , \quad (26) \\
I_{q\bar{q}} &= 1 + \frac{3\alpha_s}{2\pi^2} \ln\left(\frac{k_{Tmax}}{k_{Tmin}} \right) \left[-\frac{\pi}{9}(\delta R_2^2 - \delta R_1^2) + \xi(\delta R_2,\ \delta R_1) \right] \ , \quad (27)
\end{aligned}
$$

expressed in terms of the function[3]

$$
\xi(\delta R_2,\ \delta R_1) = \int_{\delta R_1}^{\delta R_2} d\delta R \ \delta R \int_0^{2\pi} d\phi \, \frac{\cosh(\delta R \cos\phi)}{\cosh(\delta R \cos\phi) + \cos(\delta R \sin\phi)} \, . \quad (28)
$$

A general comment is in order here. The quantitative predictions on the magnitude of the colour flow are based on the hypothesis of Local Parton Hadron Duality [16], which assumes that colour coherence effects survive the hadronization stage; an hypothesis well confirmed by existing data [17].

2.3 Photon fragmentation contribution.

The result (24) should be adequate for the $V = W,\ Z,\ H$ cases. For the γ+jet case though, we should add the contribution from processes where the final state photon comes from the fragmentation of a quark or gluon. Although such processes are formally of higher order in QCD, they may occasionally turn out to be quite important, since the logarithmic growth of the fragmentation function due to scaling violations, compensates one power of α_s [12]. The contribution from such fragmentation to the γ+jet cross section arises from each partonic subprocess

$$
a(p_1) \ + \ b(p_2) \ \to \ c(p_3) \ + \ d(p_4) \ \ , \quad (29)
$$

in which the parton c fragments subsequently to a photon, through a fragmentation described by the function $D_c^{\gamma}(z, Q_f^2)$, where z denotes the fraction of the c-momentum

[3]Notice that this result depends crucially on the fact that the antenna integration region (22, 23) is chosen so that $\delta\varphi$ in (16) remains small, so that k^{μ} never goes so close to p_4^{μ}, to make the perturbative treatment unreliable; compare (16, 15).

carried by the photon. Following [10] we write the next to leading QCD order calculation of the fragmentation contribution to $pp \to \gamma$ jet as

$$\frac{d\sigma^{frag}(pp \to \gamma\ jet)}{d\tau d\bar{y} d\cos\theta^*} = \frac{\hat{s}}{2}\sum_{abcd} f_{a/p}(x_a, Q^2) f_{b/p}(x_b, Q^2) \cdot \frac{d\hat{\sigma}(ab \to cd)}{d\hat{t}} \cdot \int_{z_{min}}^{1} dz D_c^{\gamma}(z, Q_f^2) \ , \tag{30}$$

where $f_{a/p}(x_a, Q^2)$ denotes the a-parton distribution function in a proton, at a scale $Q \simeq p_T/2$. $\sum_{abcd}$ refers to the summation over the full list of subprocesses, $q(\bar{q}) + q(\bar{q}) \to q(\bar{q}) + q(\bar{q})$, $q(\bar{q}) + g \to q(\bar{q}) + g$, $q\bar{q} \to gg$, $gg \to q\bar{q}$. The expressions for the subprocess cross sections can be found in [18, 12].

In (30), Q_f denotes the scale of the fragmentation function which, according to the next to leading order calculation in [10], is determined by

$$Q_f \ = \ \frac{p_T^{\gamma} R}{\cosh\eta_{\gamma}} \ , \tag{31}$$

where η_{γ} is the photon rapidity in the laboratory frame, and p_T^{γ} its transverse momentum. In (31), $R = \sqrt{(\delta\eta)^2 + (\delta\varphi)^2}$ denotes the size of the isolation cone around the photon produced from the c-fragmentation, within which the hadronic energy E_{had} is constrained to be smaller than some $\max(E_{had})$, which in turn determines also z_{min} in (30) through

$$z_{min} \ = \ 1 - \frac{\max(E_{had})}{E_c} \ . \tag{32}$$

The smaller $\max(E_{had})$ is chosen, the more isolated the photon becomes, which in turn means a smaller photon fragmentation contribution to the cross sections. In the calculations below we use $R = 0.7$ and $\max(E_{had}) \simeq 4\ GeV$ [20] in (31, 30), which means constraining the photon to be quite isolated. Using then standard leading order expressions for the various partonic cross sections in (30) [12], and the photon fragmentation fit [21]

$$zD_q^{\gamma}(z, Q_f^2) \ = \ \frac{\alpha}{2\pi}\left[e_q^2 \frac{2.21 - 1.28z + 1.29z^2}{1 - 1.63\ln(1-z)}\, z^{0.049} + 0.002(1-z)^2 z^{-1.54}\right] \ln(Q_f^2/\Lambda_{QCD}^2) \ , \tag{33}$$

$$zD_g^{\gamma}(z, Q_f^2) \ = \ \frac{\alpha}{2\pi}\, 0.0243(1-z)^{1.03} z^{-0.97} \ln(Q_f^2/\Lambda_{QCD}^2) \tag{34}$$

(with $\Lambda_{QCD}^2 = 0.04 GeV^2$), we calculate the photon fragmentation contribution to the cross sections, which should be added to the cross section in (24). It turns out that for all numerical applications presented below, $d\sigma^{frag}(pp \to \gamma\ jet)$ from (30) is always less than 10% of $d\sigma(pp \to \gamma\ jet)$ from (24).

We are aware that our estimate of the fragmentation contribution is very approximative. Nevertheless there are two basic reasons to be convinced that we are not far from a precise next to leading order calculation. Firstly, concerning photon fragmentation functions, it has been shown in [22] that, in the large z domain we probe ($z \simeq 1$), the photon fragmentation functions beyond leading order do not strongly deviate from the leading log parametrization we have used. Secondly, with respect to the choice of the scale of the fragmentation function and its relation to the isolation cone, we should admit that a fully satisfactory treatment is lacking at present [23]. In the present work we simply followed the results of [10].

2.4 The Asymmetry

The forward-backward asymmetry is defined as

$$A^V(\tau,\bar{y}) \;=\; \frac{\int_0^{1-\epsilon} d\cos\theta^* \left[\left.\frac{d\sigma(pp\to V\ jet)}{d\tau d\bar{y} d\cos\theta^*}\right|_{\theta^*} - \left.\frac{d\sigma(pp\to V\ jet)}{d\tau d\bar{y} d\cos\theta^*}\right|_{\pi-\theta^*}\right]}{\int_0^{1-\epsilon} d\cos\theta^* \left[\left.\frac{d\sigma(pp\to V\ jet)}{d\tau d\bar{y} d\cos\theta^*}\right|_{\theta^*} + \left.\frac{d\sigma(pp\to V\ jet)}{d\tau d\bar{y} d\cos\theta^*}\right|_{\pi-\theta^*}\right]} \,, \tag{35}$$

where ϵ is a small positive number serving to exclude the angular region around the beam direction, where the cross sections are not measurable, and the pertubative treatment not applicable. The V production cross section appearing in (35) is given in (10), and can be refined by including in it the gluon bremsstrahlung contribution at the antenna approximation as indicated in (24), as well as the fragmentation contribution from (30) for the photon case.

As it can be seen from (24, 30), the asymmetry $A^V(\tau,\bar{y})$ is always an antisymmetric function of $\bar{y}$. For the $V = W,\ Z,\ H$ cases, where (24) contributes (containing the leading order and the soft gluon contributions inside the integrals I_i), it can be expressed as

$$A^V(\tau,\bar{y}) \;=$$

$$\frac{\left[g(x_a)\Sigma_V(x_b) - \Sigma_V(x_a)g(x_b)\right] I_{gq} J^{V-}_{gq}}{\left[g(x_a)\Sigma_V(x_b) + \Sigma_V(x_a)g(x_b)\right] I_{gq} J^{V+}_{gq} + \widetilde{\Sigma}_V(x_a,x_b) I_{q\bar{q}} J^V_{q\bar{q}} + g(x_a)g(x_b) I_{gg} J^V_{gg}} \,. \tag{36}$$

The antenna pattern parameters appearing here, are given in (25-27), while those from the various subprocess cross sections are written as

$$J^{V-}_{gq} \;=\; \frac{1}{2}\int_0^{1-\epsilon} d\cos\theta^* \left[\frac{d\hat{\sigma}(gq\to Vq)}{d\hat{t}} - \frac{d\hat{\sigma}(qg\to Vq)}{d\hat{t}}\right] \,, \tag{37}$$

$$J^{V+}_{gq} \;=\; \frac{1}{2}\int_0^{1-\epsilon} d\cos\theta^* \left[\frac{d\hat{\sigma}(gq\to Vq)}{d\hat{t}} + \frac{d\hat{\sigma}(qg\to Vq)}{d\hat{t}}\right] \,, \tag{38}$$

$$J^{V}_{q\bar{q}} \;=\; \int_0^{1-\epsilon} d\cos\theta^* \left[\frac{d\hat{\sigma}(q\bar{q}'\to Vg)}{d\hat{t}}\right] \,, \tag{39}$$

$$J^V_{gg} \;=\; \int_0^{1-\epsilon} d\cos\theta^* \left[\frac{d\hat{\sigma}(gg\to Vg)}{d\hat{t}}\right] \;, \tag{40}$$

where of course (40) is relevant only in the Higgs case. The $\bar{y}$-antisymmetry of A^V is then obvious on the basis of (8, 36). Its direct dependence on the gluon distribution $g(x)$ is also clear in (36).

It is possible to write a corresponding formula for the A^γ case, but this time the result is more complicated, since the fragmentation contribution involves many subprocesses.

3 Sensitivity to the gluon distribution.

In principle the above asymmetries supply additional independent information on the parton distributions, and should be used together with the other usual measurements to constrain these distributions. Since these asymmetries are proportional to the gluon distribution, we would like to explore here their usefulness for constraining $g(x)$, assuming that the quark distributions have already been precisely determined by other means. Thus here, we are interested in using the above asymmetries for the various production processes in order to improve our knowledge on the gluon distribution $g(x)$, particularly in the large x region, where most of the uncertainties lie. We proceed as follows.

We first want to see what uncertainty our present ignorance of the parton distributions in general, and of the gluon distribution in particular, imply for the above asymmetry. This is done by using the existing fits for the parton distributions [1, 2, 3], which provide an estimate of the bands inside which the asymmetry may lie, for various values of the V+jet invariant mass $M = \sqrt{\hat{s}}$ and the rapidity $\bar{y}$ of the V+jet pair. These bands are given by the dotted lines in Figs.1, 2, 3, 4 for the $W^\pm$, Z, γ and H production cases respectively, while the full line determines the "averaged" asymmetry in each of these cases. In all figures we use $\epsilon = 0.05$ to cut the forward or backward V production, with respect to the c.m. angle; but the results are not sensitive to the exact magnitude of this value; (compare (35)).

In the figures we also include the antenna pattern contribution generated by a soft gluon jet "close" to the hard jet generated by the parton c; compare (16, 22, 23). This is integrated in the phase space region [13], [24]:

$$0.7 \lesssim \delta R \lesssim 1 \;,\quad 70GeV \lesssim k_T \lesssim 200GeV \quad \text{for LHC} \tag{41}$$

$$0.7 \lesssim \delta R \lesssim 1.3 \;,\quad 10GeV \lesssim k_T \lesssim 30GeV \quad \text{for Tevatron } (\sqrt{s} = 2TeV) \;. \tag{42}$$

The effect of such antenna contributions is to increase the forward and backward cross sections and the asymmetry by roughly 10%, in all cases.

For the γ production, we also include the fragmentation contribution from (30). It turns out that for the strong photon isolation constrain imposed by $\max(E_{had}) = 4GeV$ (compare (30, 32), the fragmentation contribution to the forward or backward cross sections are at the 10% level. This photon fragmentation contribution tends to decrease the asymmetry by roughly 10%.

Thus, the bands in Figs.1-4, give an estimate of the present uncertainty on these asymmetries, which is due to our present ignorance of the gluon distributions. To see what can be achieved by LHC and/or the upgraded Tevatron, we indicate on the same figures the uncertainties of a possible (future) measurement of these asymmetries, assumed to lie on the "averaged" solid line. These uncertainties include the statistical ones implied by the integrated luminosities (2 experiments with 3 years of running) of $600 fb^{-1}$ and $12 fb^{-1}$ for the LHC ($\sqrt{s} = 14\ TeV$) and the upgraded Tevatron ($\sqrt{s} = 2\ TeV$) respectively. For W and Z, we only retain leptonic decay modes with branching fractions $Br = 0.16$ and 0.09, respectively. One should notice that the Z + jet final state is experimentally very clean.

For γ and H we assume a detection efficiency of 0.8 and 0.01 respectively. However γ + jet final state suffers from a background from neutral pions, which will limit the accuracy of such a final state. The detection efficiency in the Higgs case is of course very much dependent on the value of the Higgs mass which controls the value of the branching ratios in $\gamma\gamma$, WW^*, ZZ^* etc, and the value of 0.01 is only chosen for orientation.

In the illustrations given in Figs.1-4 we have computed the statistical uncertainties taking bins of $\delta\bar{y} = \pm 0.02$ (indicated by the horizontal lines in the figures) and $\delta\tau = (\pm 300\ GeV \cdot M)/s$. Eq.(8) gives the relation between the kinematical domains ($\tau = M^2/s,\ \bar{y}$) and ($x_a,\ x_b$). Note that reducing the size of the bins would make the domain in ($x_a,\ x_b$) more restrictive, but it would simultaneously increase the statistical error.

To these statistical uncertainties we quadratically add the uncertainties implied by the present knowledge of the quark distribution functions, estimated by their spread among the various models. One should take into account that at LHC the lepton pseudorapidities from weak gauge bosons decays will provide the key to measure the q, $\bar{q}$ distribution functions within an accuracy of $\simeq 1\%$ [11]. The resulting total uncertainties are indicated by the vertical error bars at the central point of each bin.

Figs.1-4 show the kinematical domains where the measurement of the asymmetries can provide useful constraints on $g(x)$. In order to get informations on $g(x)$ at large x, one needs measurements at large M and $\bar{y}$; compare (8). The number of events is however decreasing with M and $\bar{y}$. For LHC we see that asymmetries for W and γ production are useful (i.e. at the percent level) for $M \lesssim 1000\ GeV$ and $|\bar{y}| \lesssim 2$, which means x values up to $x \simeq 0.3$. The results for Z production are given in Fig.2. The expected sensitivity to $g(x)$ is weaker than in the W, γ cases and it can be useful only up to $x \simeq 0.1$. The Higgs case is shown in Fig.4. One cannot expect an improvement on the determination of $g(x)$ from it, but it can contribute to consistency checks, particularly with respect to excluding possible New Physics contributions.

For the upgraded Tevatron the lower energy ($\sqrt{s} = 2TeV$) and the lower luminosity forces us to restrict to $M \lesssim 200GeV$, for which we could reach useful information (at the percent level) only for $x \lesssim 0.1$ and only from γ production (compare Fig.3), the W case giving only consistency checks.

4 Conclusions

In this paper we have shown that forward-backward asymmetries with respect to the subprocess c.m. scattering angle in V+jet production at hadron colliders, are directly proportional to the gluon distribution function $g(x)$. We have then studied how measurements of these asymmetries can improve our knowledge of this gluon distribution.

We have considered V+jet production at the upgraded Tevatron and at the LHC, for the cases $V = W^{\pm}, Z, \gamma$ and H. In order to make our treatment more realistic, we have added to the leading V+jet cross section, the contribution from the soft gluon emission in the form of an antenna pattern distribution. In the case of the photon we have also added the photon fragmentation contribution arising from the various subprocesses involving two body scattering among quarks and gluons.

We have made an estimate of the accuracy at which these asymmetries can be measured at the upgraded Tevatron and at the LHC in several bins of V+jet invariant mass and c.m. rapidity. Each bin corresponds to a certain domain in the fraction of momentum x carried by the partons. We have given the kinematical domains where this accuracy would allow a substantial improvement in the knowledge of the gluon distribution $g(x)$. More explicitly:

- At the upgraded Tevatron ($\sqrt{s} = 2\ TeV$, with an integrated luminosity of 12 fb^{-1}) and using mainly the γ+jet process, one can expect to reach an accuracy of the percent level up to about $x \simeq 0.1$.

- At LHC ($\sqrt{s} = 14\ TeV$, with an integrated luminosity of 600 fb^{-1}), mainly through the γ+jet and W+jet processes (and at a weaker level the Z+jet one) one should test $g(x)$ at less than one percent up to $x \simeq 0.3$.

- A comparison of the results in the various modes, including the H+jet one (which is by itself not accurate enough to severely constrain $g(x)$) should give consistency checks and constrain possible non standard contributions. In this respect, the radiation antenna pattern may also help.

The present study should just be taken as "a stone to be used for the construction of the building". Obviously the experimental information provided by these asymmetries should be inserted in a global analysis involving all other observables and all parton distributions. In this context it should be remembered that the information contained in these asymmetries arises from subprocess-terms which are completely different from those determining the present prompt photon [7, 8] and the dijet production cross sections at the Tevatron [25]. The simple-minded analysis presented here was just aimed at showing the peculiar role of these asymmetries for the purpose of determining the gluon distribution function, provided - as it will be the case in future hadronic colliders - high statistics will allow to take into account this forward backward asymmetry in a global analysis.

Appendix: Parton expressions for V production at a pp Collider.

For **H** production the relevant quark distribution to be used in (10, 24) are

$$\Sigma_H(x) \quad = \Sigma(x) = \sum_q \left[q(x,Q^2) + \bar{q}(x,Q^2)\right] \quad , \tag{A.1}$$

$$\widetilde{\Sigma}_H(x_a,x_b) \quad = \sum_q \left[q(x_a,Q^2)\bar{q}(x_b,Q^2) + \bar{q}(x_a,Q^2)q(x_b,Q^2)\right] \quad , \tag{A.2}$$

where the sum is over all light quark flavours. The subprocess cross sections can be found in [19, 14]. Note that the gluon-gluon term in (10) contributes only for Higgs production, and it should be ignored in the ($W,\ Z,\ \gamma$) cases below.

For **W** production ($\mathbf{W} \equiv W^+ + W^-$)

$$\Sigma_W(x) \ = \ \Sigma(x) \quad , \tag{A.3}$$

$$\begin{aligned}\widetilde{\Sigma}_W(x_a,x_b) \ &= \ d(x_a,Q^2)\bar{u}(x_b,Q^2) + \bar{u}(x_a,Q^2)d(x_b,Q^2) + \bar{d}(x_a,Q^2)u(x_b,Q^2) \\ &+ \ u(x_a,Q^2)\bar{d}(x_b,Q^2) + [u \to c \quad , \quad d \to s] \ ,\end{aligned} \tag{A.4}$$

provided we neglect the CKM matrix elements $V_{td},\ V_{ts}$. The corresponding subprocess cross sections, to leading order in QCD, are

$$\frac{d\hat{\sigma}(q\bar{q}' \to Wg)}{d\hat{t}} \ = \ \frac{\alpha_s\sqrt{2}G_F M_W^2}{4\hat{s}^2}\ \frac{8}{9}\ \frac{\hat{t}^2+\hat{u}^2+2M_W^2\hat{s}}{\hat{t}\hat{u}} \ , \tag{A.5}$$

$$\frac{d\hat{\sigma}(gq \to Wq')}{d\hat{t}} \ = \ \frac{\alpha_s\sqrt{2}G_F M_W^2}{4\hat{s}^2}\ \frac{1}{3}\ \frac{\hat{s}^2+\hat{u}^2+2M_W^2\hat{t}}{-\hat{s}\hat{u}} \ , \tag{A.6}$$

$$\frac{d\hat{\sigma}(qg \to Wq')}{d\hat{t}} \ = \ \frac{\alpha_s\sqrt{2}G_F M_W^2}{4\hat{s}^2}\ \frac{1}{3}\ \frac{\hat{s}^2+\hat{t}^2+2M_W^2\hat{u}}{-\hat{s}\hat{t}} \ . \tag{A.7}$$

Correspondingly, for **Z** production

$$\Sigma_Z(x) \ = \ \sum_q (g_{Lq}^2 + g_{Rq}^2)\left[q(x,Q^2) + \bar{q}(x,Q^2)\right] \quad , \tag{A.8}$$

$$\widetilde{\Sigma}_Z(x_a,x_b) \ = \ \sum_q (g_{Lq}^2 + g_{Rq}^2)\left[q(x_a,Q^2)\bar{q}(x_b,Q^2) + \bar{q}(x_a,Q^2)q(x_b,Q^2)\right] \quad , \tag{A.9}$$

where the Z-couplings to the L and R quarks $g_{Lq} = t_q^{(3)} - e_q s_W^2$ and $g_{Rq} = -e_q s_W^2$, are absorbed to the definition of the $\Sigma_Z,\ \widetilde{\Sigma}_Z$ distributions. In this normalization, the corresponding subprocess cross sections are given by (A.5-A.7), after replacing $M_W \to M_Z$.

Finally for **γ** production we have

$$\Sigma_\gamma(x) \ = \ \sum_q e_q^2\left[q(x,Q^2) + \bar{q}(x,Q^2)\right] \quad , \tag{A.10}$$

$$\widetilde{\Sigma}_\gamma(x_a, x_b) \;=\; \sum_q e_q^2 \left[q(x_a, Q^2)\bar{q}(x_b, Q^2) + \bar{q}(x_a, Q^2) q(x_b, Q^2) \right] \quad . \tag{A.11}$$

Since the square of the quark charge e_q^2 has been inserted in the definition (A.10, A.11), it is removed from the subprocess cross sections, which is thus written to leading QCD order as

$$\frac{d\hat{\sigma}(q\bar{q} \to \gamma g)}{d\hat{t}} \;=\; \frac{\pi \alpha_s \alpha}{\hat{s}^2} \; \frac{8}{9} \; \frac{\hat{t}^2 + \hat{u}^2}{\hat{t}\hat{u}} \,, \tag{A.12}$$

$$\frac{d\hat{\sigma}(gq \to \gamma q)}{d\hat{t}} \;=\; \frac{\pi \alpha_s \alpha}{\hat{s}^2} \; \frac{1}{3} \; \frac{\hat{s}^2 + \hat{u}^2}{-\hat{s}\hat{u}} \,, \tag{A.13}$$

$$\frac{d\hat{\sigma}(qg \to \gamma q)}{d\hat{t}} \;=\; \frac{\pi \alpha_s \alpha}{\hat{s}^2} \; \frac{1}{3} \; \frac{\hat{s}^2 + \hat{t}^2}{-\hat{s}\hat{t}} \,. \tag{A.14}$$

References

[1] A.D. Martin, R.G. Roberts, W.J. Stirling and R.S. Thorne, hep-ph/9803445.

[2] J. Huston *et.al.*, hep-ph/9801444; H.L. Lai *et.al.* Phys. Rev. **D55** (1997) 1280.

[3] M. Glück, E. Reya and A. Vogt, hep-ph/9806404.

[4] J.F. Gunion, H.E. Haber, G.L. Kane and S. Dawson, "The Higgs Hunter Guide", Addison-Wesley, Reading MA, 1990.

[5] S. Dawson, Nucl. Phys. **B359** (1991) 283; hep-ph/9703387.

[6] A. Panitch, in proceedings of the XXXIst Rencontres de Moriond, 96 QCD and High Energy Hadronic Interactions, ed J. Tran Thanh Van, eds Frontières, p 349.

[7] WA70 collaboration: M. Bonesini *et.al.* Z. f. Phys. **C38** (1988) 371.

[8] E706 collaboration: L. Apanasevich *et.al.* hep-ex/9711017.

[9] E. L. Berger, R. Meng and J. Qiu, in proceedings of the 26th Int. Conf. on High-Energy Physics, DALLAS HEP 1992 p 853.

[10] L.E. Gordon and W. Vogelsang Phys. Rev. **D50** (1994) 1901, Phys. Rev. **D52** (1995) 58.

[11] M. Dittmar, F. Pauss and D. Zurcher, Phys. Rev. **D56** (1997) 7284.

[12] See *e.g.* R.K. Ellis, W.J. Stirling and B.R. Webber, "QCD and Collider Physics", Cambridge University Press, Cambridge 1996; Yu.L. Dokshitzer, V.A. Khoze, A.H. Mueller and S.I. Troyan, "Basics of Perturbative QCD", ed. J. Tran Thanh Van, Editions Frontières, Gif-sur-Yvette 1991.

[13] V.A. Khoze and W.J. Stirling, Z. f. Phys. **C76** (1997) 59.

[14] G.J. Gounaris, J. Layssac and F.M. Renard, hep-ph/9803422, to appear in Phys. Rev. D.

[15] J. Ellis, V. Khoze and W. J. Stirling, Z. f. Phys. **C75** (1997) 287; M. Heyssler and W. J. Stirling, Phys. Lett. **B407** (1997) 407.

[16] Y. Azimov, Y. Dokshitzer, V. Khoze and S. Troyan, Z. f. Phys. **C27** (1985) 65, Z. f. Phys. **C31** (1986) 213.

[17] V. Khoze and W. Ochs, Int. J. Mod. Phys. **A12** (1997) 312.

[18] R. K. Ellis and J. Sexton, Nucl. Phys. **B269** (1986) 445.

[19] I. Hinchliffe and S.F. Novaes, Phys. Rev. **D38** (1988) 3475; R.P. Kauffman, Phys. Rev. **D44** (1991) 1415; R.K. Ellis, I. Hinchliffe, M.Soldate and J.J. van der Bij, Nucl. Phys. **B297** (1988) 221; M. Spira, A. Djouadi, D. Graudens and P.M. Zerwas, Nucl. Phys. **B453** (1995) 17; M. Spira and P.M. Zerwas, Lectures at Internazionale Unversitätswochen für Kern- und Teilchenphysik, Schladming 1997, hep-ph/9803257; M. Spira, hep-ph/9705337.

[20] ATLAS Collaboration, F. Gianotti and I. Vichou, ATLAS-PHYS-N0-78.

[21] J.F. Owens, Rev. Mod. Phys. **59** (1987) 465.

[22] L. Bourhis, M. Fontannaz and J. Ph. Guillet, Eur.Phys. J. **C2** (1998) 529.

[23] E. Pilon, in proceedings of the XXXIst Rencontres de Moriond, 96 QCD and High Energy Hadronic Interactions, ed J. Tran Thanh Van, eds Frontières, p 189.

[24] ATLAS collaboration, S. Khulmann et al, ATLAS-PHYS-N0-106.

[25] F. Abe *et.al.*, CDF collaboration, Phys. Rev. Lett. **77** (1996) 438; B. Flaughter, talk given at APS meeting, Indianapolis, May 1996; D0 collaboration: J. Blazey, talk at Rencontre de Moriond March 1996; D. Elvira, talk at Rome Conference in DIS and Related Phenomena.

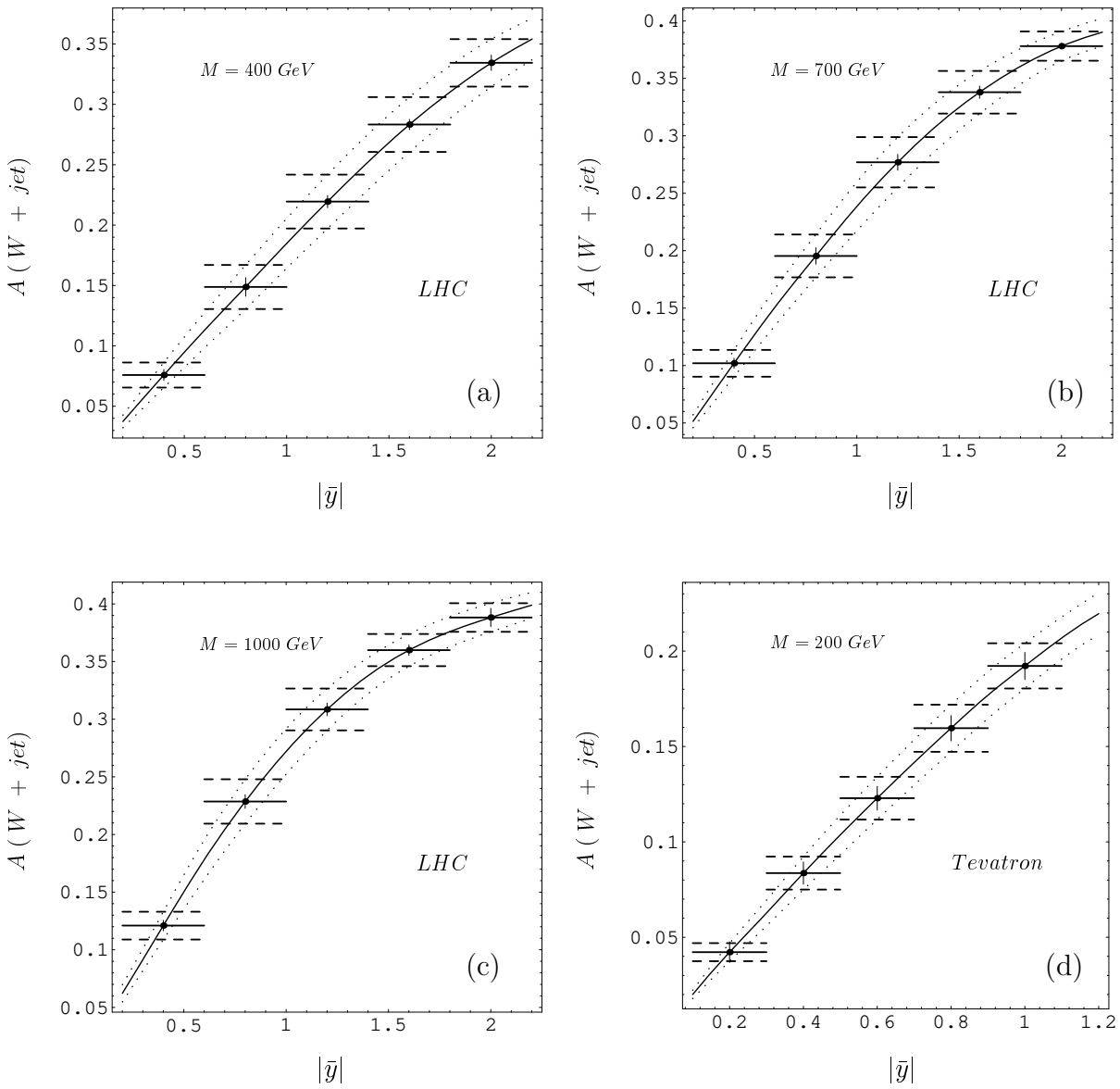

Figure 1: Asymmetry for W+jet production with invariant mass M, as a function of the pair rapidity $\bar{y}$, for LHC (a,b,c) and the upgraded Tevatron (d). The band between the two dotted lines is due to the present uncertainty on the gluon distribution function. The solid line is the center of the band. The error bar shows the accuracy at which the asymmetry can be measured for each indicated bin (dashed lines) taking into account statistical errors and uncertainties on quark distribution functions.

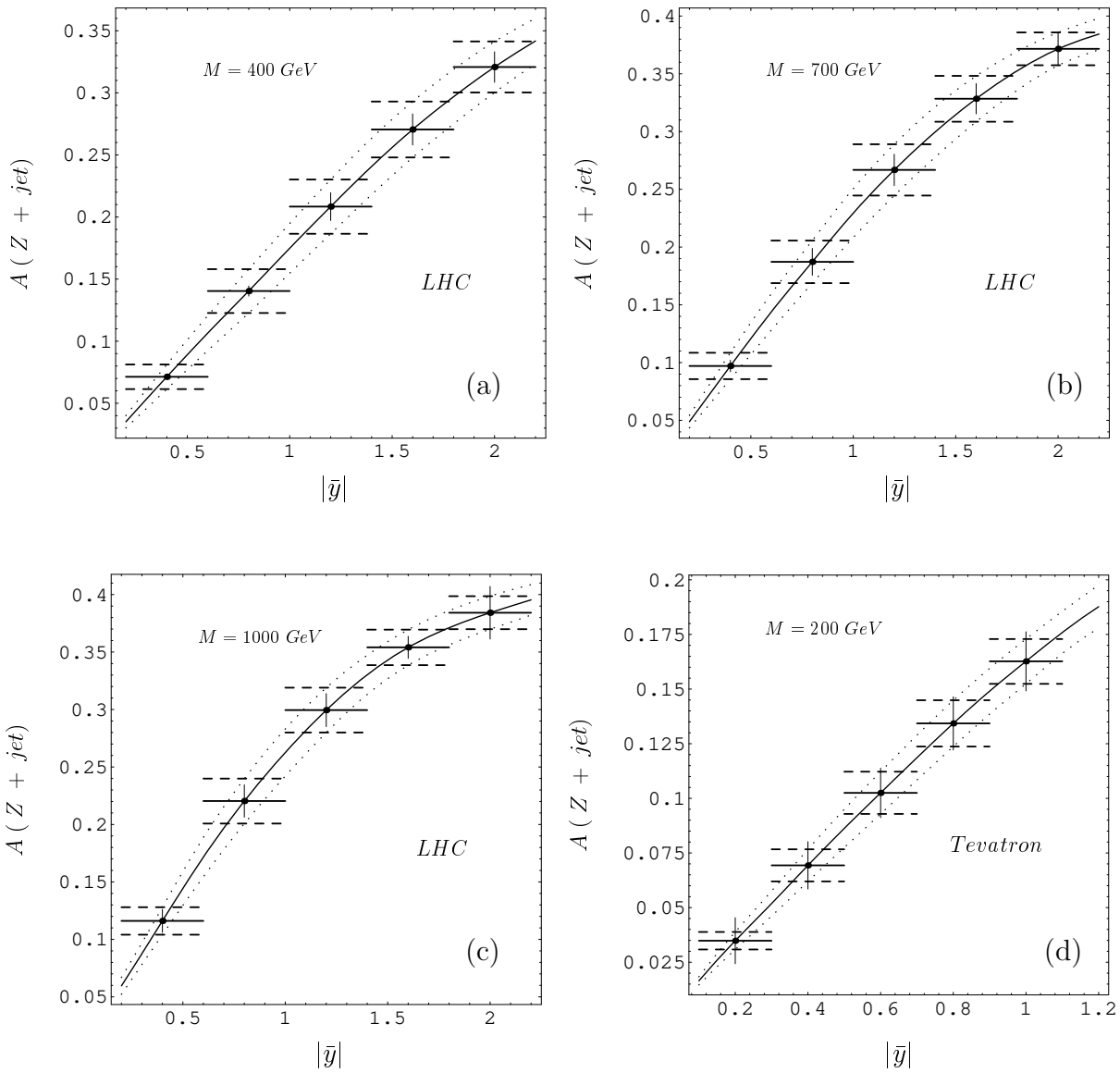

Figure 2: Asymmetry for Z+jet production with invariant mass M, as a function of the pair rapidity $\bar{y}$, for LHC (a,b,c) and the upgraded Tevatron (d). Same caption as in Fig.1.

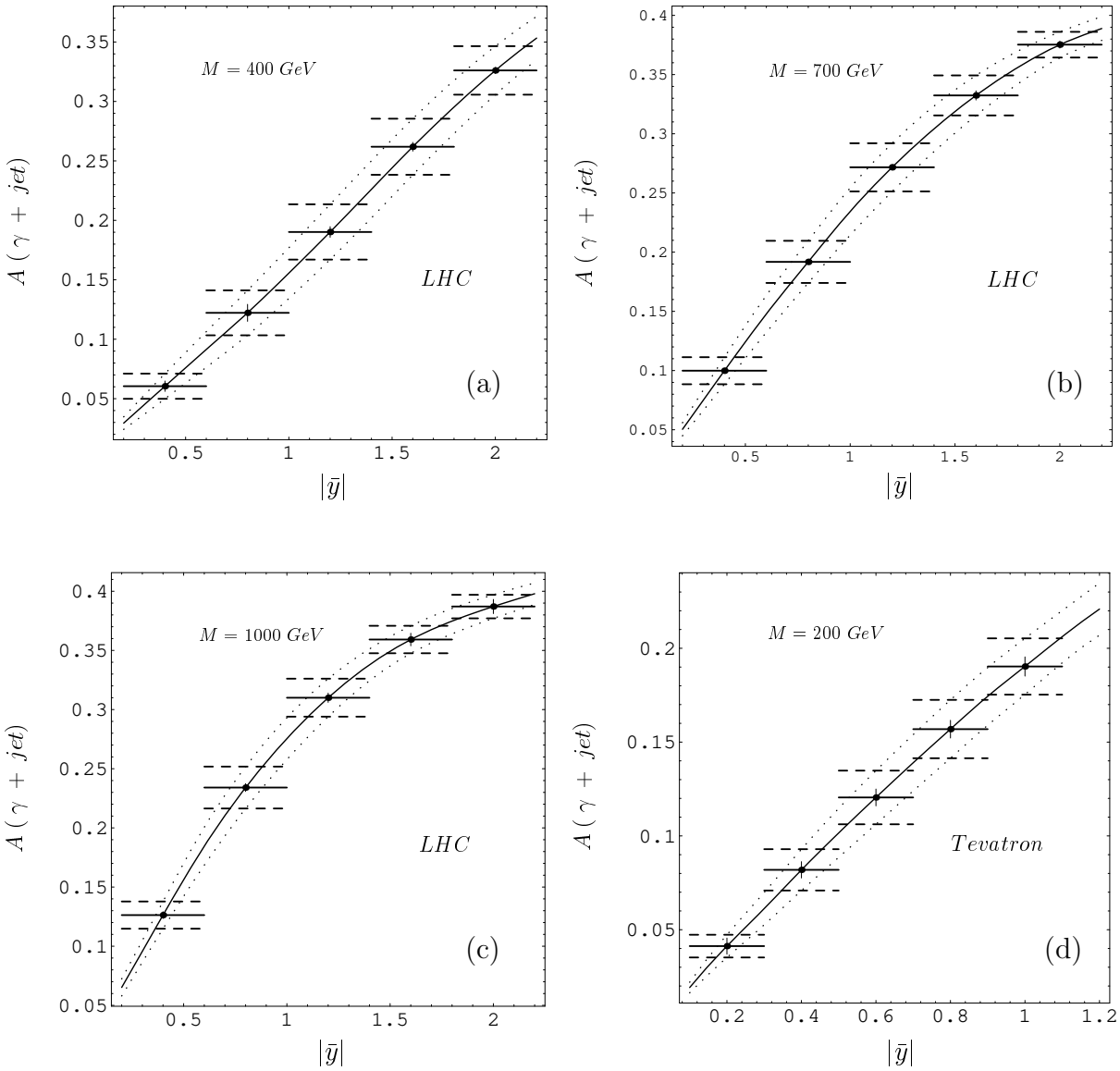

Figure 3: Asymmetry for γ+jet production with invariant mass M, as a function of the pair rapidity $\bar{y}$, for LHC (a,b,c) and the upgraded Tevatron (d). Same caption as in Fig.1.

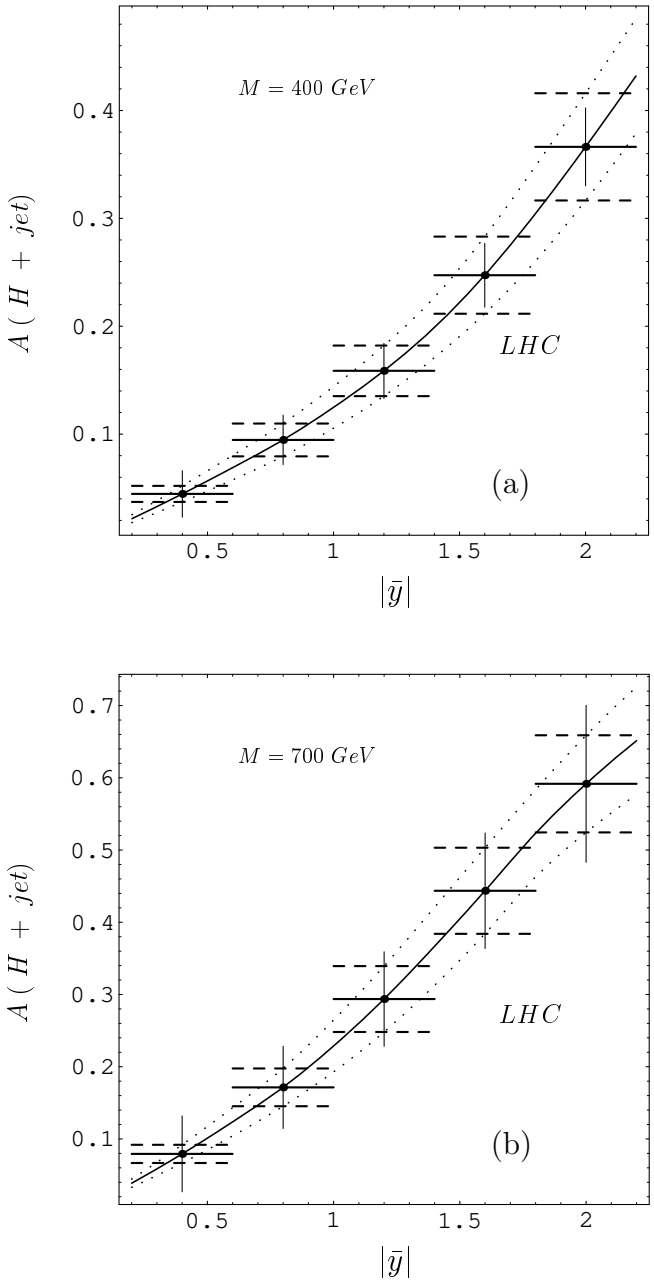

Figure 4: Asymmetry for H+jet production with invariant mass M, as a function of the pair rapidity $\bar{y}$, for LHC (a,b). Same caption as in Fig.1.